

See discussions, stats, and author profiles for this publication at: <https://www.researchgate.net/publication/338837231>

# Synthesis, characterization and antibacterial activity studies of new 2-pyrral-L-amino acid Schiff base palladium (II) complexes

Article · January 2020

DOI: 10.1007/s11696-019-00986-5

CITATION

1

READS

93

4 authors:



**Eunice Nyawade**

Jomo Kenyatta University of Agriculture and Technology

14 PUBLICATIONS 45 CITATIONS

[SEE PROFILE](#)



**Martin O. Onani**

University of the Western Cape

97 PUBLICATIONS 390 CITATIONS

[SEE PROFILE](#)



**Samantha Meyer**

Cape Peninsula University of Technology

5 PUBLICATIONS 27 CITATIONS

[SEE PROFILE](#)



**Phumuzile Dube**

University of the Western Cape

3 PUBLICATIONS 12 CITATIONS

[SEE PROFILE](#)

Some of the authors of this publication are also working on these related projects:



Cyclopentadienyl)dicarbonylruthenium(II) Amine complexes in medicine and catalysis [View project](#)



Quantum mechanical investigation of advanced solar and electronics materials [View project](#)



# Synthesis, characterization and antibacterial activity studies of new 2-pyrral-L-amino acid Schiff base palladium (II) complexes

Eunice A. Nyawade<sup>1</sup> · Martin O. Onani<sup>3</sup> · Samantha Meyer<sup>2,3</sup> · Phumuzile Dube<sup>2,3</sup>

Received: 29 May 2019 / Accepted: 30 October 2019  
© Institute of Chemistry, Slovak Academy of Sciences 2020

## Abstract

Three new 2-pyrral amino acid Schiff base palladium (II) complexes were synthesized, characterized and their activity against six bacterial species was investigated. The ligands: Potassium 2-pyrrolidine-L-methioninate (L1), Potassium 2-pyrrolidine-L-histidinate (L2) and Potassium 2-pyrrolidine-L-tryptophanate (L3) were synthesized and reacted with dichloro(1,5-cyclooctadiene)palladium(II) to form new palladium (II) complexes C1, C2 and C3, respectively. <sup>1</sup>H NMR, FTIR, UV–Vis, elemental analysis and conductivity measurements were used to characterize the products. The antibacterial activities of the compounds were evaluated against Gram-positive *Staphylococcus aureus* (*S. aureus*, ATCC 25923), methicillin-resistant *Staphylococcus aureus* (MRSA, ATCC 33591), *Staphylococcus epidermidis* (*S. epidermidis*, ATCC 12228) and *Streptococcus pyogenes* (*S. pyogenes*, ATCC 19615) and, gram-negative *Pseudomonas aeruginosa* (*P. aeruginosa*, ATCC 27853) and *Klebsiella pneumoniae* (*K. pneumoniae*, ATCC 13883) using the agar well diffusion assay and microtitre plate serial dilution method. The palladium complexes were active against the selected bacteria with the imidazole ring containing complex C2 and indole heterocyclic ring containing complex C3 showing the highest activity.

**Keywords** Schiff bases · Antibacterial · Palladium · Chelates · Amino acids · Pyrrole · Imidazole · Indole

## Introduction

The increased resistance of pathogenic bacteria to antibiotics is alarming, hence the need for new classes of antibacterial agents (Theuretzbacher 2011). These new antibacterial agents should ideally be able to evade the bacterial resistance mechanisms. The discovery and successful application

of cis-diamminedichloroplatinum(II) complex as an anticancer agent triggered research interests in the development of transition metal-based therapeutic agents (Rosenberg et al. 1969). Platinum group metal complexes have gained immense popularity as possible antibacterial agents (Kapdi and Fairlamb 2014; Wilson and Lippard 2014; Zeng et al. 2017). Research has shown that coordination of biologically active organic molecules to transition metals give a range of coordination geometries which provide more stereochemical orientations than what is possible with organic molecules, thus aiding in their specific biomolecule recognition and interaction (Chohan et al. 1997; Nyawade et al. 2015; Selvakumar et al. 2006; You et al. 2008). For instance, a palladium complex of tetracycline was reported to be 15 times more potent against *Escherichia coli*, which is resistant to tetracycline, than the free tetracycline (Guerra et al. 2005). The antimicrobial activities of palladium(II) and platinum(II) complexes have been shown against selected bacterial strains. Such complexes have also been shown to be more active than the free, uncoordinated ligands (Radic et al. 2012; Samota and Seth 2010).

Schiff bases have exhibited a wide range of biological activities which include antimicrobial (AlAjmi et al. 2016;

---

This work was presented at the International Conference on Coordination and Bioinorganic Chemistry held in Smolenice on June 2–7, 2019.

✉ Eunice A. Nyawade  
enyawade@jkuat.ac.ke

- <sup>1</sup> Department of Chemistry, University of the Western Cape, Robert Sobukwe Road, Private Bag X17, Bellville 7535, South Africa
- <sup>2</sup> Department of Biological Sciences, Faculty of Health and Wellness Sciences, Cape Peninsula University of Technology, 1906, Bellville 7535, South Africa
- <sup>3</sup> DST/Mintek Nanotechnology Innovation Centre - Biolabels Node, Department of Biotechnology, University of the Western Cape, Robert Sobukwe Road, Bellville 7535, South Africa

Karamunge and Vibhute 2013; Keypour et al. 2013; Tabassum et al. 2013; Yao et al. 2007), anticancer (Kapdi and Fairlamb 2014; Sztanke et al. 2013; Tabassum et al. 2013; Yan et al. 2015)\_ENREF\_6, anti-inflammatory, (Asif and Husain 2013; Coskun et al. 2013), antiretroviral (Sridhar et al. 2001), anticonvulsive (Abu-Surrah and Kettunen 2006) and antipyretic activities (AlAjmi et al. 2016). The presence of a lone pair of electrons in the  $sp^2$  orbital of the nitrogen atom in the azomethine group,  $-C=N-$ , of the Schiff bases is of chemical, biological and physical importance (Patai 1970). The biological activity of the Schiff bases is attributed to the formation of hydrogen bonds between the active centers of cell constituents and the  $sp^2$  hybridized orbital of the azomethine nitrogen atom (Abdel-Rahman et al. 2017, 2019; Abu-Dief and Mohamed 2015; Kabak et al. 1999). Schiff bases are generally easy to synthesize, derivatize and have good donor abilities. These compounds are, thus, suitable drug candidates. Amino acid Schiff bases are specifically very effective chelating ligands bearing carboxylate,  $COO^-$  and azomethine  $-C=N-$  groups which readily coordinate to various transition metal ions, forming chemically and thermally stable metal complexes (Grünwald et al. 2010)\_ENREF\_9. The formation of palladium chelates through the use of amino acid Schiff bases is likely to enhance their stability and improve their structural lability. Chelation by the Schiff bases reduces the metal ion polarity and increase delocalization of the  $\pi$ -electrons over the chelate ring (Ali et al. 2015) resulting in the formation of Schiff base transition metal chelates that exhibit useful physiological and pharmacological activities. These activities are due to the enhanced lipophilicity of the central metal (Ali et al. 2015; Patai 1970). There is, therefore, great interest in the bioactivities of Schiff base transition metal complexes because their coordination to transition metal ions enable them to enter target cells and enhance their biological activities (Crans et al. 2013; Nagesh et al. 2015). Amino acid Schiff base metal chelates are a new category of potential antifungal, antiviral, antibacterial and antitumor agents (Abdel-Rahman et al. 2016, 2017, 2019; Abu-Dief and Mohamed 2015; Wei et al. 2011).

The amino acid, L-histidine, has an imidazole tail which accounts for many of its biochemical activities. Imidazole and its derivatives have occupied a unique place in the field of medicinal chemistry by improving pharmacokinetic properties of lead molecules. Imidazole derivatives have broad spectrum pharmacological properties and have exhibited good antimicrobial, anticancer, analgesic and anxiolytic properties (Adinolfi et al. 2015; Desai et al. 2014; Eicher 1998; Khalid et al. 2005; Ramagiri et al. 2015; Kadavakollu et al. 2014, Verma 2013). The amino acid L-tryptophan has an indole nucleus, a generally accepted pharmacophore in medicinal compounds, which has shown some biological activities such as anti-inflammatory and analgesic, antifungal, antibacterial, insecticidal, anticancer, HIV inhibitory,

antioxidant, antitubercular, antiviral, antidepressant, tranquilizing and anticonvulsant, and antihistamine (Singh and Singh 2018). Compounds that contain imidazole and indole are of interest in medicinal chemistry due to their pharmacological and therapeutic activities.

Palladium (II) chelates are more effective anticancer agents than other metal chelates including platinum because they enable the metal to interact directly with the target deoxyribonucleic acid (DNA) molecule (Das and Livingstone 1978). On the contrary, platinum (II) chelates are kinetically inert, while metals such as nickel (II), zinc (II), and copper (II) are thermodynamically unstable (Garoufis et al. 2009). Palladium (II) ions readily form complexes with amino acids, proteins, DNA and other macromolecules such as vitamin B6 (Rîmbu et al. 2014). The structural stability and lability of palladium complexes make palladium (II) the metal of choice in the search for therapeutic metals. Furthermore, it has been shown that palladium compounds are not mutagenic and from this perspective is, therefore, safe for application in therapeutics (Melber 2002). However, the biological activity of palladium complexes of amino acid Schiff bases has not been greatly studied. Therefore, the aim of this study was to synthesize, characterize and assess the antibacterial activity of three new palladium (II) complexes of amino acid Schiff bases derived from pyrrole-2-carboxaldehyde and, L-methionine, L-histidine and L-tryptophan.

## Experimental

All reactions were performed under inert conditions using Schlenk techniques. The amino acids and pyrrole-2-carboxaldehyde were purchased from Sigma Aldrich and used without further purification. Ethanol was obtained from Sigma Aldrich and dried by refluxing over magnesium turnings and iodine before use. Diethyl ether was obtained from Sigma Aldrich and dried by refluxing over sodium wire and benzophenone. Melting points were determined using a Stuart Scientific SMP 10 apparatus and are uncorrected. Solid-state Fourier Transform infrared (FT-IR) on potassium bromide (KBr) were recorded on a Perkin Elmer Spectrum Two model FT-IR Spectrophotometer ( $4000-400\text{ cm}^{-1}$ ).  $^1\text{H}$  NMR of the compounds, in deuterated dimethylsulfoxide ( $\text{DMSO-d}_6$ ) using TMS as an internal standard, was recorded at  $25\text{ }^\circ\text{C}$  on a Bruker Avance III HD Nanobay 400-MHz NMR spectrometer equipped with a 5-mm BBO probe. Electronic spectra were recorded on a Thermo Scientific Nicolet Evolution 100 Ultraviolet visible (UV-Vis) Spectrophotometer. Conductivity measurements were performed on a HANNA EC 215 Conductivity Meter. Elemental analyses were performed on a LECO CNHS-932 micro-analyzer. The metal precursor  $[\text{Pd}(\text{COD})\text{Cl}_2]$  was prepared following literature methods (Gao et al. 2014; Wiedermann et al. 2006). The amino acid

Schiff bases were synthesized by slight modification of the procedure reported in literature (Alsalmeh et al. 2016; Heinert and Martell 1962).

### Synthesis of the Schiff bases potassium pyrrole-2-carbal amino acidate, L

An ethanolic solution of pyrrole-2-carboxaldehyde (1.0 mmol, 5.0 mL) was added to a solution of the amino acid (L-methionine (L1), L-histidine (L2) and L-tryptophan (L3) in KOH<sub>(aq)</sub>) (1.0 mmol, 5.0 mL)/ethanol (5.0 mL) mixture. The resultant mixture was stirred under reflux for 6–8 h. The mixture was cooled and filtered to remove any unreacted amino acid. A yellow to orange filtrate was removed by vacuum suction and an orange to dark brown residual solid formed. The solid was re-crystallized using ethanol, washed with cold ethanol and rinsed with diethyl ether. The solid was dried under vacuum and characterized by FTIR, NMR, UV–Vis, and elemental analysis.

#### Potassium 2-pyrral-L-methioninate, L1

Yield: 74%. Color: yellow. Molecular formula: C<sub>10</sub>H<sub>13</sub>KN<sub>2</sub>O<sub>2</sub>S. Elemental analysis: Calculated: C; 45.45, H; 4.96, N; 10.60, S; 12.13%. Found: C; 45.66, H; 4.44, N; 10.94, S; 13.26%. <sup>1</sup>H NMR (320 MHz, DMSO-d<sub>6</sub>): δ 7.85 (s, N=C(H), imine), δ 6.06–6.88 (CH, Pyrrole), δ 3.52 (dd, α-CH, L-met), δ 2.37 (dd, δ-CH<sub>2</sub>, L-met), δ 1.90, 2.05 (m, β-CH<sub>2</sub>, L-met), δ 2.01 (s, S-CH<sub>3</sub>, L-met). IR (KBr, solid state; cm<sup>-1</sup>): ν(HC=N) 1597, ν(COO<sup>-</sup>)<sub>asym</sub> 1418, ν(COO<sup>-</sup>)<sub>sym</sub> 1358, ν(S–C) 744. UV–Vis: λ<sub>max</sub> (nm) (DMSO): 288, 328, 433. Mpt: 269 °C.

#### Potassium 2-pyrral-L-histidinate, L2

Yield: 23.3% yield. Color: orange. Molecular formula: C<sub>11</sub>H<sub>11</sub>KN<sub>4</sub>O<sub>2</sub>. Elemental analysis: Calculated: C; 56.89, H; 5.21, N; 23.28%. Found: C; 56.06, H; 5.92, N; 22.84%. <sup>1</sup>H NMR (320 MHz, DMSO-d<sub>6</sub>): δ 7.82 (s, N=C(H), imine), δ 7.11–7.43 (N–C(H)=C, imidazole), δ 6.83–6.05 (C(H), Pyrrole), δ 3.14 (dd, α-CH, L-hist), δ 3.67, 2.92 (m, β-CH<sub>2</sub>, L-hist). IR (KBr, solid state; cm<sup>-1</sup>): ν(HC=N) 1622, ν(COO<sup>-</sup>)<sub>asym</sub> 1412, ν(COO<sup>-</sup>)<sub>sym</sub> 1345. UV–Vis: λ<sub>max</sub> (nm) (DMSO): 288, 325, 436. Mpt: 255 °C.

#### Synthesis of potassium 2-pyrral-L-tryptophanate, L3

Yield: 41% yield. Color: orange. Molecular formula: C<sub>16</sub>H<sub>14</sub>KN<sub>3</sub>O<sub>2</sub>. Elemental analysis: Calculated: C; 60.17, H; 4.42, N; 13.16%. Found: C; 59.08, H; 4.83, N; 13.66%. <sup>1</sup>H NMR (320 MHz, DMSO-d<sub>6</sub>): δ 7.78 (s, N=C(H), imine), δ 7.55–6.85 (benzyl C(4H), indole), δ 6.91–6.29, 6.02 (CH, Pyrrole), δ 3.83 (dd, α-CH, L-trypt), δ 3.39, 3.30 (m, β-CH<sub>2</sub>,

L-hist), δ 7.00 (N=C(H)–N, Indole). IR (KBr, solid state; cm<sup>-1</sup>): ν(HC=N) 1622, ν(COO<sup>-</sup>)<sub>asym</sub> 1398, ν(COO<sup>-</sup>)<sub>sym</sub> 1354. UV–Vis: λ<sub>max</sub> (nm) (DMSO): 220, (282, 289), 329, 436. Mpt: 113 °C.

### Synthesis of the 2-pyrral-L-amino acid palladium(II) complexes C1, C2 and C3, [PdLCl]2H<sub>2</sub>O

A solution of dichloro(1,5-cyclooctadiene)palladium(II) (157.0 mg; 0.55 mmol) in 5.0-mL dry dichloromethane was added dropwise to an equimolar ethanolic solution of the Schiff base (L1, L2 and L3) (5 mL) in a clean dry Schlenk tube. The mixture was stirred at 25 °C temperature for 6 h. A dark orange precipitate was formed. The mixture was filtered and the residue was washed with cold methanol and rinsed with diethyl ether. The solid was dried under reduced pressure and characterized using FTIR, <sup>1</sup>H NMR, UV–Vis and elemental analysis.

#### 2-pyrral-L-methionine palladium(II) complex, C1 [PdL1Cl]2H<sub>2</sub>O

Molecular formula: C<sub>10</sub>H<sub>17</sub>ClN<sub>2</sub>O<sub>4</sub>PdS. Elemental analysis: Calculated: C; 29.79, H; 4.24, N; 6.95, S; 7.95%. Found: C; 29.49, H; 3.9, N; 6.33, S; 7.51%. <sup>1</sup>H NMR (320 MHz, MeOD): δ 8.32 (s, N=C(H), imine), δ 7.21–6.06 (C(H), Pyrrole), δ 4.02 (dd, α-CH, L-met), δ 3.39 (H, H<sub>2</sub>O), δ 3.25 (dd, δ-CH<sub>2</sub>, L-met), δ 2.63, 2.06 (m, β-CH<sub>2</sub>, L-met), δ 2.06 (s, S-CH<sub>3</sub>, L-met). IR (KBr, solid state; cm<sup>-1</sup>): ν(OH–O) 3450, ν(OC=O) 1726.1, ν(HC=N) 1578, ν(COO<sup>-</sup>)<sub>asym</sub> 1418, ν(COO<sup>-</sup>)<sub>sym</sub> 1316, ν(S=C) 1210, ν(S–C) 751, ν(M–O) 588, ν(M–N) 433. UV–Vis: λ<sub>max</sub> (nm) (DMSO): 302, 338, 374, 444, 522. Mpt: 150 °C.

#### 2-pyrral-L-histidine palladium(II) complex, C2 [PdL2Cl]2H<sub>2</sub>O

Molecular formula: C<sub>11</sub>H<sub>15</sub>ClN<sub>4</sub>O<sub>2</sub>Pd. Elemental analysis: Calculated: C; 32.29, H; 3.70, N; 13.69%. Found: C; 33.01, H; 3.62, N; 13.11%. <sup>1</sup>H NMR (320 MHz, DMSO-d<sub>6</sub>): δ 12.76 (N(H), imidazole), δ 9.47 (C=C(H)–N, imidazole), 8.13 (N=C(H), imine), 7.12 (s, N–C(H)=C, imidazole), δ 7.2, 7.0, 6.28 (CH, Pyrrole), δ 4.40 (dd, α-CH, L-hist), δ 5.0, 2.93 (m, β-CH<sub>2</sub>, L-hist), δ 3.37 (H, H<sub>2</sub>O). IR (KBr, solid state; cm<sup>-1</sup>): ν(OH–O) 3424, ν(OC=O) 1723.8, ν(HC=N) 1608, ν(COO<sup>-</sup>)<sub>asym</sub> 1418, ν(COO<sup>-</sup>)<sub>sym</sub> 1309, ν(M–O) 622, ν(M–N) 447. UV–Vis: λ<sub>max</sub> (nm) (DMSO): 303, 378, 459, 518. Mpt > 250 °C.

#### 2-pyrral-L-tryptophan palladium(II) complex, C3 [PdL3Cl]2H<sub>2</sub>O

Molecular formula: C<sub>16</sub>H<sub>18</sub>ClN<sub>3</sub>O<sub>2</sub>Pd. Elemental analysis: Calculated: C; 49.91, H; 3.96, N; 19.94%. Found: C; 50.01,

H; 3.55, N; 20.32%.  $^1\text{H}$  NMR (320 MHz, DMSO- $d_6$ ):  $\delta$  9.33 (NH, Pyrrole),  $\delta$  11.05 (s, N(H), indole),  $\delta$  8.21 (s, N=C(H), imine),  $\delta$  7.23 (N-C(H)=C, indole),  $\delta$  7.58–7.00 (CH, Pyrrole),  $\delta$  4.14 (dd,  $\alpha$ -CH, L-trypt),  $\delta$  3.37 (O(H), H<sub>2</sub>O),  $\delta$  2.29 (m,  $\beta$ -CH<sub>2</sub>, L-hist),  $\delta$  7.58–77.00 (CH, indole). IR (KBr, solid state;  $\text{cm}^{-1}$ ):  $\nu(\text{OH}-\text{O})$  3453,  $\nu(\text{OC}=\text{O})$  1735.43,  $\nu(\text{HC}=\text{N})$  1608,  $\nu(\text{COO}^-)$  asym, 1411,  $\nu(\text{COO}^-)$  sym 1342,  $\nu(\text{M}-\text{O})$  598,  $\nu(\text{M}-\text{N})$  430. UV-Vis:  $\lambda_{\text{max}}$  (nm) (DMSO): 290, 335, 382, 482, 522. Mpt: 170 °C.

### Evaluation of antibacterial activity

The antibacterial activity of the amino acid Schiff bases and their metal complexes were tested against *Staphylococcus epidermidis* (SE), *Pseudomonas aeruginosa* (PA), *Streptococcus pyogenes* (SP), *Klebsiella pneumoniae* (KP), Methicillin-resistant *Staphylococcus aureus* (MRSA) and *Staphylococcus aureus* (SA) using the agar well diffusion assay (Rahman et al. 2015). The lowest concentration of the samples that inhibits the visual growth of the bacteria, i.e., the minimum inhibitory concentration (MIC) was also determined in micro-dilution (Balouiri et al. 2016). Microbial suspensions in Mueller–Hinton broth were incubated for 24 h at 37 °C, from which a McFarland No. 0.5 standard at a spectrophotometric wavelength of 625 nm was prepared.

### Agar well diffusion assays

Solutions of the synthesized ligands L1, L2 and L3, and their respective palladium complexes C1, C2 and C3 (10 mg/mL) were prepared by dissolving in 10% DMSO. Mueller–Hinton agar was inoculated with the respective test microorganisms (inoculum size:  $1 \times 10^8$  CFU/ml of bacteria) (Balouiri et al. 2006). Holes (6 mm in diameter) were punched into the agar plates using a sterile cork borer and 50  $\mu\text{l}$  of the respective sample solution were introduced into each well. The broad spectrum antibiotic ampicillin was used as the positive control while 10% DMSO was used as the negative control. The plates were then incubated at 37 °C for 24 h. The inhibition zones were measured in millimeters (mm) from the circumference of the well to that of the growth-free zones around

the disk (Table 1). All samples were tested in triplicate (Rahman et al. 2015).

### Minimum inhibitory concentration (MIC)

The MIC for each sample was determined using the microtiter plate method (Balouiri et al. 2016). Mueller–Hinton broth was inoculated with single colonies of bacterial strains and incubated for 24 h at 37 °C. A McFarland No. 0.5 bacterial suspension was prepared and further diluted as described by Balouiri, et al. (Balouiri et al. 2016). Ampicillin, a broad spectrum antibiotic, was used as a positive control (to confirm microbial susceptibility). DMSO (10%) served as the negative control. In a laminar flow cabinet, 96-well microtiter plates were aseptically prepared as follow. The ligand and complexes were dissolved in 10% DMSO (DMSO was diluted using the respective broth) to starting concentrations of 2.5 mg/ml. In each well of the microtiter plate, 100  $\mu\text{l}$  of broth was added except for the first wells in which 200  $\mu\text{l}$  of the ligand/broth or complex/broth solution was added. Two-fold serial dilutions were made across the plate, such that the full range of concentrations tested was 0.0049–2.5 mg/ml. The respective bacterial suspensions were added to the wells except to one well, which was used as the background interference standard. The plates were incubated for 24 h at 37 °C. After incubation, the absorbance reading at 625 nm, for each plate, was recorded on a POLARstar Omega spectrophotometer (BMG labtech, Germany). The MIC determined by the spectrophotometric method was defined as the concentration at which there was a sharp decline in the absorbance value after incubation (Devienne and Raddi 2002). Growth inhibition was confirmed by visual inspection of the wells.

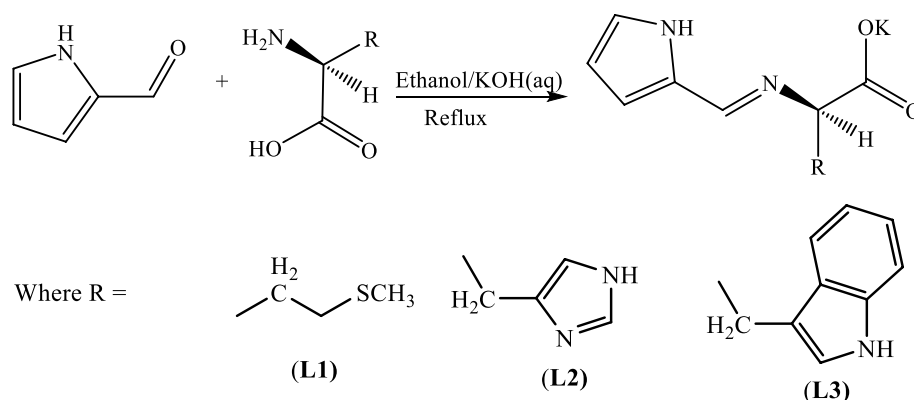
## Results and discussion

### Synthesis and characterization of the Schiff base

The Schiff base ligands L1, L2 and L3 were synthesized by condensation of pyrrole-2-carboxaldehyde with the amino

**Table 1** Infrared and proton NMR data for the ligands and complexes

Compound	FTIR $\text{cm}^{-1}$							$^1\text{H}$ NMR ppm	
	$\nu(\text{H}_2\text{O})$	$\nu(\text{OC}=\text{O})$	$\nu(\text{HC}=\text{N})$	$\nu(\text{COO}^-)$ asym	$\nu(\text{COO}^-)$ sym	$\nu(\text{M}-\text{O})$	$\nu(\text{M}-\text{N})$	$\delta(\text{H}-\text{C}=\text{N})$	$\delta(\text{H}-\text{OH})$
L1	–	–	1597	1418	1358	–	–	7.85	–
C1	2450	1726	1578	1418	1316	588	455	8.32	3.39
L2	–	–	1622	1412	1345	–	–	7.88	–
C2	3424	1724	1608	1418	1309	622	477	8.13	3.37
L3	–	–	1633	1398	1356	–	–	7.78	–
C3	3453	1735	1625	1411	1342	598	430	8.21	3.37

**Scheme 1** Synthesis of L-amino acid Schiff base ligands L1, L2 and L3**Table 2** Elemental analysis and UV–Vis data

Compound	Molecular weight (g/mol)	Elemental analysis				UV–Vis ( $\lambda_{\text{max}}$ , nm)	Melting point $^{\circ}\text{C}$
		C	H	N	S		
L1 $\text{C}_{10}\text{H}_{13}\text{KN}_2\text{O}_2\text{S}$	264.38	45.66 (45.45)	4.44 (4.96)	10.94 (10.60)	13.26 (12.13)	205, 288, 328, 433,	269
C1 $\text{C}_{10}\text{H}_{17}\text{ClN}_2\text{O}_4\text{PdS}$	403.19	29.79 (29.49)	4.25 (3.90)	6.95 (6.33)	7.95 (7.51)	302, 338, 374, 444, 522	150
L2 ( $\text{C}_{11}\text{H}_{11}\text{KN}_4\text{O}_2$ )	270.33	56.06 (56.89)	5.92 (5.21)	22.84 (23.28)		205, 288, 325, 436	255
C2 $\text{C}_{11}\text{H}_{15}\text{ClN}_4\text{O}_4\text{Pd}$	409.14	32.29 (33.01)	3.70 (3.62)	13.69 (13.11)		303, 378, 459, 518	–
L3 ( $\text{C}_{16}\text{H}_{14}\text{KN}_3\text{O}_2$ )	319.41	59.08 (60.17)	4.83 (4.42)	13.66 (13.16)		203, 220, (282, 289), 329, 436	113
C3 $\text{C}_{16}\text{H}_{18}\text{ClN}_3\text{O}_4\text{Pd}$	458.21	49.91 (50.01)	3.96 (3.55)	19.94 (20.32)		290, 335, 382, 482, 522	170

acids L-methionine, L-histidine and L-tryptophan, respectively, in the ration of 1:1 (Scheme 1).

The Schiff bases, pale yellow-to-orange solids, are air and moisture sensitive, soluble in water, methanol, ethanol and DMSO, but insoluble in non-polar solvents. The infrared and NMR data of the ligands and complexes are provided in Table 1.

Strong vibration frequencies assignable to the  $\nu(\text{HC}=\text{N})$  were observed at  $1597\text{ cm}^{-1}$ ,  $1622\text{ cm}^{-1}$  and  $1633\text{ cm}^{-1}$  for ligands L1, L2 and L3, respectively. The  $\nu(\text{HC}=\text{N})$  vibrations are at a lower frequency than that observed for the carbonyl group of pyrrole-2-carboxaldehyde,  $\nu(\text{HC}=\text{O})$  at  $1639\text{ cm}^{-1}$ , a clear indication that the azomethine group replaced the carbonyl group during the Schiff base ligand formation (Abu-Dief and Mohamed 2015, Arish and Nair 2012). The asymmetric carboxylate stretching bands  $\nu_{\text{asym}}(\text{COO}^-)$  were observed in the range  $1418\text{--}1398\text{ cm}^{-1}$  while the symmetric stretching band  $\nu_{\text{sym}}(\text{COO}^-)$  was observed in the range  $1347\text{--}1361\text{ cm}^{-1}$  (Rîmbu et al. 2014). The  $\nu(\text{C}\text{--}\text{S})$  band was observed at  $744\text{ cm}^{-1}$  for ligand L1.

Formation of the Schiff base was further confirmed by the presence of a strong singlet peak at 7.75–7.85 ppm, in  $^1\text{H}$  NMR spectrum, assignable to the azomethine proton,  $\text{H}\text{--}\text{C}=\text{N}$ . The absence of the carbonyl proton  $\text{H}\text{--}\text{C}=\text{O}$  signal (9.80 ppm) from the spectrum of the Schiff bases further confirmed the formation of the Schiff base. The pyrrole

**Table 3** Conductivity values for the metal complexes in DMSO

Metal complexes	[Pd(L1)Cl] $2\text{H}_2\text{O}$	[Pd(L2)Cl] $2\text{H}_2\text{O}$	[Pd(L3)Cl] $2\text{H}_2\text{O}$	DMSO
Conductivity mS/cm	0.24	0.23	0.20	0.25

proton signals were observed in the range 6.08–6.88 ppm. The elemental analysis data (Table 2) are consistent with the calculated values, a further proof that the Schiff base was synthesized.

The UV–Vis absorption bands (Table 3) for the ligands were observed at; 282–290 nm assignable to  $\pi\text{--}\pi^*$  transitions in the pyrrole rings,  $\sim 325\text{--}329\text{ nm}$  assignable to  $\pi\text{--}\pi^*$  transitions in the azomethine bond and  $\sim 433\text{--}436\text{ nm}$  assignable to  $n\text{--}\pi^*$  transition for the azomethine.

### Synthesis and characterization of the metal complexes

The metal complexes (Fig. 1) were synthesized by the reaction of the pyrrole-2-amino acid Schiff bases with  $[\text{Pd}(\text{COD})\text{Cl}_2]$  in the ratio of 1:1 at room temperature (Scheme 2).

The metal complexes were obtained as orange to dark brown solids soluble in DMSO, DMF, ethanol and methanol



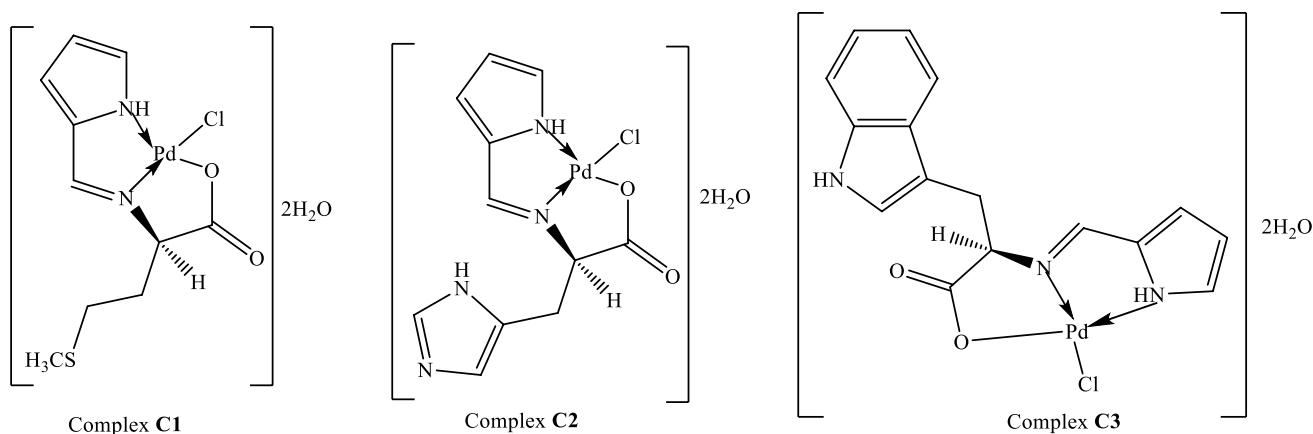
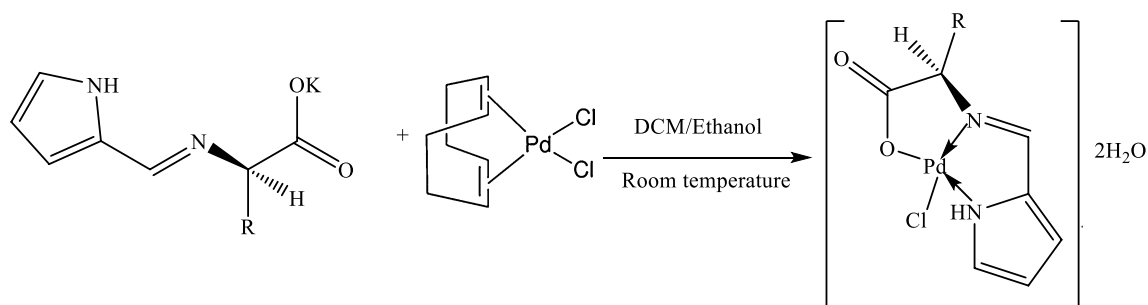


Fig. 1 Structure of the complexes C1, C2 and C3



Scheme 2 Synthesis of the palladium(II) L-amino acid Schiff base complexes

but insoluble in non-polar solvents such as chloroform and methylene chloride. The metal complexes were characterized by FTIR, UV-Vis,  $^1\text{H}$ NMR and elemental analysis (Tables 2 and 3). The IR spectrum of the complexes showed strong bands in the range  $1578\text{--}1625\text{ cm}^{-1}$  associated with the  $\nu(\text{C}=\text{N})$  stretch. The  $\nu(\text{C}=\text{N})$  stretching frequencies appeared lower than that observed for the free Schiff base ligands by approximate  $22\text{ cm}^{-1}$ . This is most likely a result of coordination to the metal via the electron rich azomethine nitrogen (Abdel-Rahman et al. 2019; Abu-Dief and Mohamed 2015). The electron density on the azomethine bond decreases; hence,  $\pi$  character decreases, the bond order decreases and the  $\text{C}=\text{N}$  bond strength decreases. The carboxylate group symmetric stretch,  $\nu(\text{OC}-\text{O}^-)_{\text{sym}}$ , shifted to lower frequency compared to the free ligand, a sign of coordination to the metal center via the carboxylate ion. This is a probable sign that there is less resonance upon coordination of the Schiff base to the metal center via the negatively charged end of the carboxylate ion. It is worth noting that new bands associated with carboxylic acid  $\nu(\text{OC}=\text{O})_{\text{asym}}$  stretch, absent in the ligand IR spectrum, were observed at  $1735\text{--}1724\text{ cm}^{-1}$ . This observation also suggests decrease in resonance as a result of coordination via the electron

rich negatively charged oxygen ( $\text{O}^-$ ) of the carboxylate ion. The large difference of about  $200\text{ cm}^{-1}$  between the  $\nu(\text{OC}-\text{O}^-)_{\text{sym}}$  and  $\nu(\text{OC}=\text{O})_{\text{asym}}$  vibrations is an indicator of the monodentate binding nature of the carboxylate group in the complexes (Arish and Nair 2012; Deacon and Phillips 1980; Nakamoto et al. 1961). New bands assignable to  $\nu(\text{M}-\text{O})$  and  $\nu(\text{M}-\text{N})$  stretching vibrations were observed at  $588\text{ cm}^{-1}$  and  $433\text{ cm}^{-1}$ , respectively (Arish and Nair 2012; Nakamoto et al. 1961; Ouf et al. 2010). The metal-oxygen and metal-nitrogen bond stretching vibrations are conclusive evidence of coordination via oxygen of the carboxylate and nitrogen of the azomethine groups. The infrared analysis suggests that the Schiff bases are coordinated to the metal ion via nitrogen and oxygen atoms. The presence of a strong, broad peak in the IR spectra of the complexes in the region  $3400\text{--}3500\text{ cm}^{-1}$  is assignable to water molecules associated with the complexes.

The proton NMR data further confirmed the coordination mode of the Schiff bases to the metal center. The azomethine proton NMR peak shifted downfield to  $8.1\text{--}8.32\text{ ppm}$  compared to the free ligand peak at  $7.78\text{--}7.98\text{ ppm}$ . The azomethine proton is more deshielded in the metal complex as the  $\pi$  character of the  $\text{C}=\text{N}$  bond

increases on coordination to the metal center. The  $\alpha$ -CH protons signal in the metal complex shifted downfield as electrons are pushed towards the nitrogen atom for coordination. No signal was observed for the pyrrole NH proton in both the ligands and their corresponding complexes. A slight up-field shift of about 0.5 ppm was observed on the pyrrole CH protons of the complexes with respect to the free ligand. This observation suggests coordination of the ligand to the metal via the nitrogen atom of the pyrrole ring. It is worth noting that a broad sharp peak was observed at 3.2 ppm in all the complexes, a sign that water is probably associated with the palladium complexes.

The UV–Vis absorption bands in the complexes for the azomethine C=N bonds observed at  $\sim$ 338 nm were assigned to the  $\pi$ - $\pi^*$  transitions and 378–389 nm assigned to the  $n$ - $\pi^*$  transitions, a Bathochromic shift with respect to absorptions observed for the free ligands (Ali et al. 2006; Biyala et al. 2008). This is an indication that coordination of the ligands to the metal center occurred via the azomethine nitrogen atom. The UV absorption band associated with the pyrrole  $n$ - $\pi^*$  transitions is observed at 303 nm, a bathochromic shift with respect to the absorptions observed in the ligand. This suggests that the ligand is probably coordinated to the metal via the pyrrole nitrogen. Ligand to metal charge transfer can be assigned the strong bands observed at 444–459 nm in the metal complexes (Biyala et al. 2008). The LMCT supports bonding via the oxygen atom of the carboxylate group. New absorption bands were appeared in the regions 378–382 nm and 518–522 nm. Palladium (II) with  $4d^8$  electronic configuration is expected to exhibit a square planar geometry associated with the three d–d transitions;  $^1A_{1g} \rightarrow ^1A_{2g}$  (463–522 nm),  $^1A_{1g} \rightarrow ^1B_{1g}$  (405–418 nm) and  $^1A_{1g} \rightarrow ^1E_g$  (344–386 nm) (Lever 1984). It is worth noting that the electronic spectra of palladium(II) complexes, in which a chalcogen is coordinated to the metal, are complicated since tails of strong O  $\rightarrow$  M LMCT band extends into the visible section of the spectrum thereby masking the expected d–d transition bands (Ali et al. 2006). However, in this study, bands observed in the regions 518–522 nm, 444–459 nm and 374–382 nm of the electronic spectra of the complexes can be assigned to  $^1A_{1g} \rightarrow ^1A_{2g}$ ,  $^1A_{1g} \rightarrow ^1B_{1g}$  and  $^1A_{1g} \rightarrow ^1E_g$ , respectively (Biyala et al. 2008).

Conductivity measurements of solutions the metal complexes in DMSO were the same as that observed for pure DMSO (Table 3). This is an indication that the complexes are neutral non-electrolytes with coordinated chloride.

The palladium(II) complexes can, therefore, be assigned a square planar geometry based on the UV–Vis, IR and NMR spectra. Each ligand is coordinated to the palladium(II) ion in a tridentate manner with a chloride ion occupying the fourth position and two water molecules associated with the complexes as water of hydration outside the coordination sphere. The spectroscopic data suggest that the ligand

**Table 4** Average zones of inhibition (mm  $\pm$  SD) produced for the ligands and their palladium complexes

Microbial strains	Zones of inhibition (mm $\pm$ SD)							Statistical significance						
	L1	Cl <sup>a</sup>	L2	C2 <sup>b</sup>	L3	C3 <sup>c</sup>	[CODPdCl <sub>2</sub> ] <sup>d</sup>	Ampicillin	ab	ac	ad	bc	bd	cd
SE	0.0 $\pm$ 0	17.78 $\pm$ 0.035	0.0 $\pm$ 0	17.3 $\pm$ 2.08	0.0 $\pm$ 0	29.86 $\pm$ 0	13.7 $\pm$ 0.6	23.82 $\pm$ 0.01	ns	ns	ns	ns	ns	ns
PA	–	–	–	–	–	–	–	–	ns	ns	ns	ns	ns	ns
SP	0.0 $\pm$ 0	14.56 $\pm$ 0	0.0 $\pm$ 0	14.72 $\pm$ 0.02	0.0 $\pm$ 0	23.34 $\pm$ 2.52	9.3 $\pm$ 0.6	17.24 $\pm$ 0.02	ns	ns	ns	ns	ns	ns
KP	0.0 $\pm$ 0	0.0 $\pm$ 0	0.0 $\pm$ 0	0.0 $\pm$ 0	0.0 $\pm$ 0	11.68 $\pm$ 0	9.3 $\pm$ 0.6	14.58 $\pm$ 0	ns	ns	ns	ns	ns	ns
MRSA	0.0 $\pm$ 0	16.50 $\pm$ 2.0	0.0 $\pm$ 0	16.88 $\pm$ 0	0.0 $\pm$ 0	25.22 $\pm$ 0.57	9.7 $\pm$ 1.2	17.38 $\pm$ 0	ns	ns	ns	ns	ns	ns
SA	0.0 $\pm$ 0	16.88 $\pm$ 0.11	0.0 $\pm$ 0	16.40 $\pm$ 0.11	0.0 $\pm$ 0	24.10 $\pm$ 0	13.3 $\pm$ 1.2	46.58 $\pm$ 0.05	ns	ns	ns	ns	ns	ns



**Table 5** Minimum inhibitory concentrations (MIC) results for the complexes

Compounds	Bacterial species					
	<i>S. epidermidis</i>	<i>P. aeruginosa</i>	<i>S. pyogenes</i>	<i>K. pneumoniae</i>	MRSA	<i>S. aureus</i>
C1	0.315	–	0.625	–	0.625	0.625
C2	0.078	–	0.156	–	0.156	0.156
C3	0.078	–	0.156	–	0.078	0.078
CODPdCl <sub>2</sub>	0.315	–	0.625	0.625	0.625	0.625
Ampicillin	0.04	0.02	0.02	0.63	0.31	0.02

is coordinated to the metal center via the azomethine nitrogen, the pyrrole nitrogen and O<sup>−</sup> of the carboxylate group.

### Antibacterial activity

Preliminary antibacterial activity of the ligands L1, L2 and L3, and their respective palladium (II) complexes C1, C2 and C3 was performed against *Staphylococcus epidermidis* (SE), *Pseudomonas aeruginosa* (PA), *Streptococcus pyogenes* (SP), *Klebsiella pneumoniae* (KP), *Methicilin Resistant Staphylococcus aureus* (MRSA) and *Staphylococcus aureus* (SA) using the agar well diffusion assay. The diameters of the zones of inhibitions are tabulated in Table 4.

Zones of inhibition were observed for C3 for all the bacterial strains used in this study, except for *P. aeruginosa*. Zones of inhibition were observed for C1 and C2 against all the bacterial strains except for *P. aeruginosa* and *K. pneumoniae*. *P. aeruginosa* was, thus, resistant to all the tested compounds including ampicillin. The antimicrobial activities of C1 and C2 were statistically similar; whilst C1 and C3, and C2 and C3, respectively, were significantly different against all the tested bacteria except against *P. aeruginosa*. No zones of inhibition were observed for wells containing the ligands, which suggest that the ligands did not inhibit the growth of any of the tested bacterial strains. Arish and Nair (2012) previously found that pyrrol-L-histidinate, a ligand identical to L2, demonstrated antibacterial activity against *P. aeruginosa* and *S. aureus*.

The MIC values were determined for the ligands (L1, L2 and L3) and metal complexes (C1, C2 and C3) against six bacterial strains (Table 5). The lowest MIC (0.078 mg/mL) was observed for C3 against *S. epidermidis*, *S. aureus* and MRSA. The same MIC value was obtained for C2 against *S. epidermidis*. MIC values for all the other treatments were higher than 0.078 mg/mL. The highest MIC value (0.625 mg/mL) was obtained for C1 against *S. pyogenes*, *S. aureus* and MRSA. The micro-dilution assay confirms that the *P. aeruginosa* is resistant to C1, C2 and C3, as the MIC values could not be established against this organism. Although it was shown using the disk diffusion assay that C3 was able to produce a zone of inhibition for *K. pneumoniae*,

an MIC value for C3 could not be determined against this organism. The micro-dilution assay again confirmed that *K. pneumoniae* was resistant to C1 and C2. The MIC values for the ligands were more than 2.5 mg/ml and confirm that the ligands do not have an antibacterial activity at the concentrations tested in this study.

The differences in activities of the tested complexes can be attributed to the different amino acid tails, present in the ligands. For instance, the imidazole and indole tails, which are known pharmacophores, enhanced the antibacterial activity of the complexes. Imidazole is a polar and ionisable aromatic compound that improves pharmacokinetic properties of lead molecules. The imidazole ring, for instance, is present in many antimicrobial drugs such as antifungals, nitroimidazole series of antibiotics and the sedative imidazolam. The indole nucleus, a biologically accepted pharmacophore in medicinal compounds, has shown biological activities such as anti-inflammatory and analgesic, antifungal, antimicrobial, insecticidal, anticancer, HIV inhibitor, antioxidant, antituberculosis, antiviral, antidepressant, tranquilizing and anticonvulsant, and antihistamine (Singh and Singh 2018). This explains why both complexes C2 and C3 which bear the imidazole and indole tails, respectively, are more active against the bacteria strains used in this study than complex C1 which bears an aliphatic sulfur group.

### Conclusions

The ligands L1, L2 and L3, and their respective palladium (II) complexes C1, C2 and C3 were successfully synthesized. The ligands are tridentate and are coordinated to the metal center via the pyrrole nitrogen, imine nitrogen and the amino acid anionic oxygen. The complexes showed good antimicrobial activity against the tested bacteria with complexes C3 and C2 exhibiting stronger antibacterial activity than complex C1. The amino acid tail used has a direct influence on the activity of the 2-pyrrol amino acid palladium(II) complexes. The aliphatic sulfur group (complex C1) had minimal influence while the imidazole and indole rings exhibited the best antibacterial activity at the

lowest concentrations of complexes C2 and C3. The ligands did not show any antibacterial activities against any of the bacterial species tested despite literature reports that amino acid Schiff bases are active against various bacterial species (Arish and Nair 2012). The reason for this deviation is not known.

**Acknowledgements** We would like to thank Jomo Kenyatta University of Agriculture and Technology in Kenya for granting Dr. Eunice Nyawade study leave to undertake this study at the University of the Western Cape, South Africa. We would also like to thank the UWC for allowing us to use their chemistry laboratory to do the synthesis and characterization work, and DST/Mintek Nanotechnology Innovation Centre for performing the antibacterial studies.

**Funding** This work was supported by the National Research Foundation, South Africa.

## References

- Abdel-Rahman LH, Abu-Dief AM, Ismael M, Mohamed MAA, Hashem NA (2016) Synthesis, structure elucidation, biological screening, molecular modeling and DNA binding of some Cu(II) chelates incorporating imines derived from amino acids. *J Mol Struct* 1103:232–244. <https://doi.org/10.1016/j.molstruc.2015.09.039>
- Abdel-Rahman LH, Abu-Dief AM, Aboelez MO, Hassan Abdel-Mawgoud AA (2017) DNA interaction, antimicrobial, anticancer activities and molecular docking study of some new VO(II), Cr(III), Mn(II) and Ni(II) mononuclear chelates encompassing quaridentate imine ligand. *J Photochem Photobiol B Biol* 170:271–285. <https://doi.org/10.1016/j.jphotobiol.2017.04.003>
- Abdel-Rahman LH, Abu-Dief AM, Shehata MR, Atlam FM, Abdel-Mawgoud AAH (2019) Some new Ag(I), VO(II) and Pd(II) chelates incorporating tridentate imine ligand: design, synthesis, structure elucidation, density functional theory calculations for DNA interaction, antimicrobial and anticancer activities and molecular docking studies. *Appl Organomet Chem* 33:e4699. <https://doi.org/10.1002/aoc.4699>
- Abu-Dief AM, Mohamed IMA (2015) A review on versatile applications of transition metal complexes incorporating Schiff bases. Beni-Suef University. *J Basic Appl Sci* 4:119–133. <https://doi.org/10.1016/j.bjbas.2015.05.004>
- Abu-Surrah AS, Kettunen M (2006) Platinum group antitumor chemistry: design and development of new anticancer drugs complementary to cisplatin. *Curr Med Chem* 13:1337–1357. <https://doi.org/10.2174/092986706776872970>
- Adinolfi B, Carpi S, Romanini A, Da Pozzo E, Castagna M, Costa B et al (2015) Analysis of the antitumor activity of clotrimazole on A375 human melanoma cells. *Anticancer Res* 35:3781–3786
- AlAjmi MF, Hussain A, Alsalmeh A, Khan RA (2016) In vivo assessment of newly synthesized achiral copper(II) and zinc(II) complexes of a benzimidazole derived scaffold as a potential analgesic, antipyretic and anti-inflammatory. *RSC Adv* 6:19475–19481. <https://doi.org/10.1039/C5RA25071D>
- Ali MA, Mirza AH, Butcher RJ, Crouse KA (2006) The preparation, characterization and biological activity of Palladium(II) and Platinum(II) complexes of tridentate nns ligands derived from S-methyl- and S-benzylthiocarbazates and the X-ray crystal structure of the [Pd(mpsme)Cl] complex. *Trans Metal Chem* 31:79–87. <https://doi.org/10.1007/s11243-005-6305-3>
- Ali OAM, El-Medani SM, Abu Serea MR, Sayed ASS (2015) Unsymmetrical Schiff base (ON) ligand on complexation with some transition metal ions: synthesis, spectral characterization, antibacterial, fluorescence and thermal studies. *Spectrochim Acta A Mol Biomol Spectrosc* 136:651–660. <https://doi.org/10.1016/j.saa.2014.09.079>
- Alsalmeh A, Laeeq S, Dwivedi S, Khan MS, Al Farhan K, Musarrat J et al (2016) Synthesis, characterization of  $\alpha$ -amino acid Schiff base derived Ru/Pt complexes: induces cytotoxicity in HepG2 cell via protein binding and ROS generation. *Spectrochim Acta A Mol Biomol Spectrosc* 163:1–7. <https://doi.org/10.1016/j.saa.2016.03.012>
- Arish D, Nair MS (2012) Synthesis, characterization and biological studies of Co(II), Ni(II), Cu(II) and Zn(II) complexes with pyrrol-1-histidinolate. *Arab J Chem* 5:179–186. <https://doi.org/10.1016/j.arabjch.2010.08.011>
- Asif M, Husain A (2013) Analgesic, anti-inflammatory, and antiplatelet profile of hydrazones containing synthetic molecules. *J Appl Chem* 2013:7. <https://doi.org/10.1155/2013/247203>
- Balouiri M, Sadiki M, Ibsouda SK (2016) Methods for in vitro evaluating antimicrobial activity: a review. *J Pharmaceut Anal* 6:71–79. <https://doi.org/10.1016/j.jpha.2015.11.005>
- Biyala MK, Sharma K, Swami M, Fahmi N, Singh RV (2008) Spectral and biocidal studies of palladium(II) and platinum(II) complexes with monobasic bidentate Schiff bases. *Transit Met Chem* 33:377–381. <https://doi.org/10.1007/s11243-008-9053-3>
- Chohan ZH, Praveen M, Ghaffar A (1997) Structural and biological behaviour of Co(II), Cu(II) and Ni(II) metal complexes of some amino acid derived Schiff-bases. *Met-Based Drugs* 4:267–272. <https://doi.org/10.1155/mbd.1997.267>
- Coskun MD, Ari F, Oral AY, Sarimahmut M, Kutlu HM, Yilmaz VT et al (2013) Promising anti-growth effects of palladium(II) saccharinate complex of terpyridine by inducing apoptosis on transformed fibroblasts in vitro. *Bioorg Med Chem* 21:4698–4705. <https://doi.org/10.1016/j.bmc.2013.05.023>
- Crans DC, Woll KA, Prusinskas K, Johnson MD, Norkus E (2013) Metal speciation in health and medicine represented by iron and vanadium. *Inorg Chem* 52:12262–12275. <https://doi.org/10.1021/ic4007873>
- Das M, Livingstone SE (1978) Cytotoxic action of some transition metal chelates of Schiff bases derived from S-methylthiocarbamate. *Br J Cancer* 37:466–469. <https://doi.org/10.1038/bjc.1978.68>
- Deacon GB, Phillips RJ (1980) Relationships between the carbon-oxygen stretching frequencies of carboxylate complexes and the type of carboxylate coordination. *Coord Chem Rev* 33:227–250. [https://doi.org/10.1016/S0010-8545\(00\)80455-5](https://doi.org/10.1016/S0010-8545(00)80455-5)
- Desai NC, Maheta AS, Rajpara KM, Joshi VV, Vaghani HV, Satodiya HM (2014) Green synthesis of novel quinoline based imidazole derivatives and evaluation of their antimicrobial activity. *J Saudi Chem Soc* 18:963–971. <https://doi.org/10.1016/j.jscs.2011.11.021>
- Devienne KF, Raddi MSG (2002) Screening for antimicrobial activity of natural products using a microplate photometer. *Braz J Microbiol* 33:166–168
- Eicher T, Pozharskii AF, Soldatenkov AT, Katritzky AR (1998) *Heterocycles in life and society*, 1st edn. Wiley, New York, p 301
- Gao E-J, Hong F, Zhu M-C, Ma C, Liang S-K, Zhang J et al (2014) Effect of carbon chain length on biological activity of novel palladium (II) complexes. *Eur J Med Chem* 82:172–180. <https://doi.org/10.1016/j.ejmech.2014.05.021>
- Garoufis A, Hadjikakou SK, Hadjiliadis N (2009) Palladium coordination compounds as anti-viral, anti-fungal, anti-microbial and anti-tumor agents. *Coord Chem Rev* 253:1384–1397. <https://doi.org/10.1016/j.ccr.2008.09.011>

- Grünwald KR, Saischek G, Volpe M, Belaj F, Mösch-Zanetti NC (2010) Pyridazine-based ligands and their coordinating ability towards first-row transition metals. *Eur J Inorg Chem* 2010:2297–2305. <https://doi.org/10.1002/ejic.201000120>
- Guerra W, de Andrade Azevedo E, de Souza Monteiro AR, Bucciarelli-Rodriguez M, Chartone-Souza E, Nascimento AMA et al (2005) Synthesis, characterization, and antibacterial activity of three palladium(II) complexes of tetracyclines. *J Inorg Biochem* 99:2348–2354. <https://doi.org/10.1016/j.jinorgbio.2005.09.001>
- Heinert D, Martell AE (1962) Pyridoxine and pyridoxal analogs. V. syntheses and infrared spectra of Schiff bases. *J Am Chem Soc* 84:3257–3263. <https://doi.org/10.1021/ja00876a009>
- Kabak M, Elmali A, Elerman Y (1999) Keto–enol tautomerism, conformations and structure of N-(2-hydroxy-5-methylphenyl)-2-hydroxybenzaldehydeimine. *J Mol Struct* 477:151–158. [https://doi.org/10.1016/S0022-2860\(98\)00604-8](https://doi.org/10.1016/S0022-2860(98)00604-8)
- Kadavakollu S, Stailey C, Kunapareddy CS, White W (2014) Clotrimazole as a cancer drug: a short review. *Med Chem* 4:722–724. <https://doi.org/10.4172/2161-0444.1000219>
- Kapdi AR, Fairlamb IJS (2014) Anti-cancer palladium complexes: a focus on PdX<sub>2</sub>L<sub>2</sub>, palladacycles and related complexes. *Chem Soc Rev* 43:4751–4777. <https://doi.org/10.1039/C4CS00063C>
- Karamunge KG, Vibhute YB (2013) Synthesis and antimicrobial activity of some new Schiff bases. *J Phys Conf Ser* 423:012006
- Keypour H, Shayesteh M, Rezaeivala M, Chalabian F, Elerman Y, Buyukgungor O (2013) Synthesis, spectral characterization, structural investigation and antimicrobial studies of mononuclear Cu(II), Ni(II), Co(II), Zn(II) and Cd(II) complexes of a new potentially hexadentate N<sub>2</sub>O<sub>4</sub> Schiff base ligand derived from salicylaldehyde. *J Mol Struct* 1032:62–68. <https://doi.org/10.1016/j.molstruc.2012.07.056>
- Khalid MH, Tokunaga Y, Caputy AJ, Walters E (2005) Inhibition of tumor growth and prolonged survival of rats with intracranial gliomas following administration of clotrimazole. *J Neurosurg* 103:79–86. <https://doi.org/10.3171/jns.2005.103.1.0079>
- Lever ABP (1984) *Inorganic electronic spectroscopy*. Elsevier, Amsterdam
- Melber CK, Keller D, Mangelsdorf I (2002) *Environmental Health Criteria 226: Palladium*. World Health Organization
- Nagesh GY, Mahendra Raj K, Mruthyunjayaswamy BHM (2015) Synthesis, characterization, thermal study and biological evaluation of Cu(II), Co(II), Ni(II) and Zn(II) complexes of Schiff base ligand containing thiazole moiety. *J Mol Struct* 1079:423–432. <https://doi.org/10.1016/j.molstruc.2014.09.013>
- Nakamoto K, Morimoto Y, Martell AE (1961) Infrared spectra of metal chelate compounds. IV. Infrared spectra of addition compounds of metallic acetylacetonates Ia. *J Am Chem Soc* 83:4533–4536. <https://doi.org/10.1021/ja01483a010>
- Nyawade EA, Friedrich HB, Omondi B, Chenia HY, Singh M, Gorle S (2015) Synthesis and characterization of new  $\alpha$ ,  $\alpha'$ -diaminoalkane-bridged dicarbonyl( $\eta^5$ -cyclopentadienyl) ruthenium(II) complex salts: antibacterial activity tests of  $\eta^5$ -cyclopentadienyl dicarbonyl ruthenium(II) amine complexes. *J Organomet Chem* 799–800:138–146. <https://doi.org/10.1016/j.jorganchem.2015.09.007>
- Ouf AE-F, Ali MS, Saad EM, Mostafa SI (2010) pH-metric and spectroscopic properties of new 4-hydroxysalicylidene-2-aminopyrimidine Schiff-base transition metal complexes. *J Mol Struct* 973:69–75. <https://doi.org/10.1016/j.molstruc.2010.03.037>
- Patai S (1970) *Analysis of azomethines. Carbon–Nitrogen double bonds*. Interscience, New York
- Radić GP, Glodović VV, Radojević ID, Stefanović OD, Čomić LR, Ratković ZR et al (2012) Synthesis, characterization and antimicrobial activity of palladium(II) complexes with some alkyl derivatives of thiosalicylic acids: crystal structure of the bis(S-benzyl-thiosalicylate)–palladium(II) complex, [Pd(S-bz-thiosal)2]. *Polyhedron* 31:69–76. <https://doi.org/10.1016/j.poly.2011.08.042>
- Rahman LHA, Abu-Dief AM, Hashem NA, Seleem AA (2015) Recent advances in synthesis, characterization and biological activity of nano sized Schiff base amino acid M(II) complexes. *Int J Nanomat Chem* 1:79–95
- Ramagiri RK, Thupurani MK, Vedula RR (2015) Synthesis, characterization, and antibacterial activity of some novel substituted imidazole derivatives via one-pot three-component. *J Heterocycl Chem* 52:1713–1717. <https://doi.org/10.1002/jhet.2261>
- Rîmbu C, Danac R, Pui A (2014) Antibacterial activity of Pd(II) complexes with salicylaldehyde-amino acids Schiff bases ligands. *Chem Pharmaceut Bull* 62:12–15. <https://doi.org/10.1248/cpb.c12-01087>
- Rosenberg B, Vancamp L, Trosko JE, Mansour VH (1969) Platinum compounds: a new class of potent antitumor agents. *Nature* 222:385–386. <https://doi.org/10.1038/222385a0>
- Samota MK, Seth G (2010) Synthesis, characterization, and antimicrobial activity of palladium(II) and platinum(II) complexes with 2-substituted benzoxazole ligands. *Heteroatom Chem* 21:44–50. <https://doi.org/10.1002/hc.20578>
- Selvakumar B, Rajendiran V, Uma Maheswari P, Stoeckli-Evans H, Palaniandavar M (2006) Structures, spectra, and DNA-binding properties of mixed ligand copper(II) complexes of iminodiacetic acid: the novel role of diimine co-ligands on DNA conformation and hydrolytic and oxidative double strand DNA cleavage. *J Inorg Biochem* 100:316–330. <https://doi.org/10.1016/j.jinorgbio.2005.11.018>
- Singh TP, Singh OM (2018) Recent progress in biological activities of indole and indole alkaloids. *Mini Rev Med Chem* 18:9–25. <https://doi.org/10.2174/1389557517666170807123201>
- Sridhar SK, Pandeya SN, De Clercq E (2001) Synthesis and anti-HIV activity of some isatin derivatives. *Boll Chim Farm* 140:302–305
- Sztanke K, Maziarka A, Osinka A, Sztanke M (2013) An insight into synthetic Schiff bases revealing antiproliferative activities in vitro. *Bioorg Med Chem* 21:3648–3666. <https://doi.org/10.1016/j.bmc.2013.04.037>
- Tabassum S, Asim A, Khan RA, Hussain Z, Srivastav S, Srikrishna S et al (2013) Chiral heterobimetallic complexes targeting human DNA-topoisomerase I[small alpha]. *Dalton Trans* 42:16749–16761. <https://doi.org/10.1039/C3DT51209F>
- Theuretzbacher U (2011) Resistance drives antibacterial drug development. *Curr Opin Pharmacol* 11:433–438. <https://doi.org/10.1016/j.coph.2011.07.008>
- Verma A, Joshi S, Singh D (2013) Imidazole: having versatile biological activities. *J Chem* 2013:10. <https://doi.org/10.1155/2013/329412>
- Wei Q-Y, Xiong J-J, Jiang H, Zhang C, Wen Y (2011) The antimicrobial activities of the cinnamaldehyde adducts with amino acids. *Int J Food Microbiol* 150:164–170. <https://doi.org/10.1016/j.ijfoodmicro.2011.07.034>
- Wiedermann J, Mereiter K, Kirchner K (2006) Palladium imine and amine complexes derived from 2-thiophenecarboxaldehyde as catalysts for the Suzuki cross-coupling of aryl bromides. *J Mol Catal A Chem* 257:67–72. <https://doi.org/10.1016/j.molcata.2006.04.009>
- Wilson JJ, Lippard SJ (2014) Synthetic methods for the preparation of platinum anticancer complexes. *Chem Rev* 114:4470–4495. <https://doi.org/10.1021/cr4004314>
- Yan X, Xu J, Wu X, Zhang Z, Zhang X, Fan Y et al (2015) Proteasome inhibition and cytostatic effects on human cancer cells by pyrazolone-enamines: a combined crystallographic, structural and computational study. *New J Chem* 39:2168–2180. <https://doi.org/10.1039/C4NJ01906G>

- Yao X, Panichpisal K, Kurtzman N, Nugent K (2007) Cisplatin nephrotoxicity: a review. *Am J Med Sci* 334:115–124
- You Z-L, Shi D-H, Xu C, Zhang Q, Zhu H-L (2008) Schiff base transition metal complexes as novel inhibitors of xanthine oxidase. *Eur J Med Chem* 43:862–871. <https://doi.org/10.1016/j.ejmech.2007.06.015>
- Zeng L, Gupta P, Chen Y, Wang E, Ji L, Chao H et al (2017) The development of anticancer ruthenium(ii) complexes: from single

molecule compounds to nanomaterials. *Chem Soc Rev* 46:5771–5804. <https://doi.org/10.1039/C7CS00195A>

**Publisher's Note** Springer Nature remains neutral with regard to jurisdictional claims in published maps and institutional affiliations.